Supplement for

Measurement report: Molecular characteristics of cloud water in southern China and insights into aqueous-phase processes from Fourier Transform Ion Cyclotron Resonance Mass Spectrometry

Wei Sun[1, 2], Yuzhen Fu[1, 2], Guohua Zhang[1, 3], Yuxiang Yang[1, 2], Feng Jiang[1, 2, a], Xiufeng Lian[1, 2, b], Bin Jiang[1], Yuhong Liao[1], Xinhui Bi[1, 3], Duohong Chen[4], Jianmin Chen[5], Xinming Wang[1, 3], Jie Ou[6], Ping'an Peng[1], Guoying Sheng[1]

[1] State Key Laboratory of Organic Geochemistry and Guangdong Key Laboratory of Environmental Protection and Resources Utilization, Guangzhou Institute of Geochemistry, Chinese Academy of Sciences, Guangzhou, 510640, PR China
[2] University of Chinese Academy of Sciences, Beijing, 100049, PR China
[3] Guangdong-Hong Kong-Macao Joint Laboratory for Environmental Pollution and Control, Guangzhou Institute of Geochemistry, Chinese Academy of Sciences, Guangzhou 510640, PR China
[4] State Environmental Protection Key Laboratory of Regional Air Quality Monitoring, Guangdong Environmental Monitoring Center, Guangzhou 510308, PR China
[5] Shanghai Key Laboratory of Atmospheric Particle Pollution and Prevention, Department of Environmental Science and Engineering, Fudan University, Shanghai 200433, PR China
[6] Shaoguan Environmental Monitoring Center, Shaoguan 512026, PR China
[a] now at: Institute of Meteorology and Climate Research, Karlsruhe Institute of Technology, Eggenstein-Leopoldshafen 76344, Germany
[b] now at: Institute of Mass Spectrometry and Atmospheric Environment, Guangdong Provincial Engineering Research Center for On-line Source Apportionment System of Air Pollution, Jinan University, Guangzhou 510632, PR China

Correspondence to: Xinhui Bi (bixh@gig.ac.cn)

Text S1. Sample collection and pretreatment

Cloud water for FT-ICR MS analysis was sampled during May 11 to 12 (Table 1). A Caltech Active Strand Cloud Water Collector, Version 2 (CASCC2) was used for sample collection (Demoz et al., 1996). Cloud events were identified using the temperature and humidity sensors and the visibility meter in a co-working ground-based counterflow virtual impactor (Model 1205, Brechtel Mfg., Inc., USA), according to the following criteria: visibility ≤ 3 km, relative humidity ≥ 95%, and no precipitation. During sampling, cloud droplets entered the collector powered by a rear fan, and condensed on a bank of Teflon strands at a flow rate of 5.8 m^3 min^{-1} and a collection efficiency of 86%. Condensed cloud water flowed into the per-cleaned sample jar through a Teflon tube equipped at the bottom of the collector. The pH of the cloud water was measured using a pH meter. Samples were refrigerated immediately after sampling and kept until the analysis. The cloud liquid water content (LWC) during the sampling was calculated as follows (Guo et al., 2012):

$$\mathrm{LWC} = \Delta m/(\Delta t \times \eta \times Q)$$

where Δm represents the mass of the sample (g); Δt represents the sampling interval (min). η is the collection efficiency, which was regarded as 86% for cloud droplets larger than 3.5 μm; and Q is the air flow of the CASCC2, i.e., 5.8 m^3 min^{-1}.

For FT-ICR MS analysis, water-soluble organic compounds in cloud water were isolated using solid-phase extraction (SPE) (Zhao et al., 2013; Bianco et al., 2018). The SPE cartridges (Strata-X, Phenomenex) were pre-conditioned sequentially with 3 mL of isopropanol, 6 mL of acetonitrile, 6 mL of methanol containing 0.1% of formic acid, and 6 mL of ultrapure water containing 0.1% formic acid. Then, 40 mL of cloud water without pH adjustment was added to the cartridge at a flow rate of approximately 1 mL min^{-1}. The inorganic salts were removed from the cartridge using 4 mL of ultrapure water containing 0.1% formic acid. Note that some low-weight organic molecules are expected to be lost in this step. The cartridge was then freeze-dried, and the analytes were eluted using 3 mL of acetonitrile/methanol/ultrapure water (45/45/10, *v:v:v*) at pH 10.4, with the pH being adjusted using ammonium hydroxide. All the solvents were HPLC-grade. A blank sample was processed and analyzed following the same procedure.

Text S2. Sample collection of interstitial $PM_{2.5}$

Whatman quartz fiber filters were used to collected $PM_{2.5}$ samples at the same site using a $PM_{2.5}$ sampler (PM-PUF-300, Mingye Inc., China) at a flow rate of 300 L min^{-1}. The sampling interval of $PM_{2.5}$ was roughly 24 hours. Two samples of $PM_{2.5}$ were collected within two days (P1: May 11 10:14-May 12 9:48, P2: May 12 10:15-May 13 10:15, respectively) during the investigated cloud events. The samples were stored at -20 ℃ immediately after sampling. For the laboratory analysis, 60 cm^2 of the sample filters were cut into pieces and soaked in ultra-clean water. Then the water soluble organic matter in $PM_{2.5}$ were separated into the ultra-clean water by 30 min ultrasonic extraction for three times, after that the extract was filtered using 0.22 μm polytetrafluoroethylene filter. The extract was then pretreated and analyzed used the same methods of cloud water samples.

Text S3. Instrumental analysis and data processing

A solariX XR FT-ICR MS instrument (Bruker Daltonik GmbH, Bremen, Germany) equipped with a 9.4-T refrigerated, actively shielded superconducting magnet (Bruker Biospin, Wissembourg, France) and a Paracell analyzer cell was used in this study. Samples were ionized using an ESI ion source (Bruker Daltonik GmbH, Bremen, Germany) in the negative ion mode. The detected mass range for FT-ICR MS was set to *m/z* 150-1000. The ion accumulation time was set to 0.1 s. A total of 128 continuous 4M data FT-ICR transients were co-added to enhance the signal-to-noise ratio and dynamic range. A typical mass-resolving power ($m/\Delta m50\%$, where $\Delta m50\%$ is the magnitude of the mass spectral peak full width at half-maximum peak height) of more than 450,000 at *m/z* 319 with a <0.3 ppm absolute mass error was achieved. The mass spectra was calibrated externally using measurements of a known homologous series of N_1 (neutral nitrogen compounds) and O_2 compounds (acids) with high abundance in a petroleum sample. The final spectrum was internally recalibrated with typical class species peaks using quadratic calibration in DataAnalysis 5.0 (Bruker Daltonics) followed the methods of Shi et al. (2012): when a peak was assigned to a molecular formula, it was used as a reference for assignment for other peaks with consecutive mass interval. For example, the formulas that differ only in the number of alkyl groups exhibit the same Kendrick mass defects and would be searched automatically. All the mathematically possible formulas for all the ions with a signal-to-noise ratio greater than 10, considering a mass tolerance of ±0.6 ppm were calculated. The maximum numbers of atoms for the formula calculator were set to: 30 ^{12}C, 60 ^{1}H, 20 ^{16}O, 2 ^{14}N, 2 ^{32}S, 1 ^{13}C, 1 ^{18}O, and 1 ^{34}S. Formulas assigned to isotopomers (i.e., ^{13}C, ^{18}O or ^{34}S) were not discussed in this study. Thus, the chemical formula $C_cH_hO_oN_nS_s$ was obtained. Future selecting was applied using following criteria to exclude formulas not detected frequently in natural materials: $O/C \leq 1.2$, $0.3 \leq H/C \leq 2.25$, $N/C \leq 0.5$, $S/C \leq 0.2$, $2C + 2 > H$, $C + 2 > O$ and obeying N rule. Finally, only intensities of sample ion peaks enhanced at least 100 times higher than those in the blank were retained for further data analysis in order to avoid possible contamination. The double-bond equivalent (DBE) can be used to evaluate the number of rings and double bonds in a molecule (An et al., 2019). The DBE of each assigned molecular formula ($C_cH_hO_oN_nS_s$) was calculated as follows:

$$\mathrm{DBE} = (2c + 2 - h + n)/2$$

The oxidation state of carbon atoms (OS_C) was calculated as followes based on the approximation described in Kroll et al. (2011); Brege et al. (2018):

$$OS_C \approx 2*o/c - h/c - 5*n/c - 6*s/c$$

The modified aromaticity index (AI_{mod}) was first proposed by Koch et al. to evaluate the aromaticity of high-resolution mass data (Koch and Dittmar, 2006):

$$AI_{mod} = (1 + c - 0.5*o - s - 0.5*h)/(c - 0.5*o - s - n)$$

$AI_{mod} \geq 0.5$ and 0.67 represent the existence of aromatic and condensed aromatic structures (Koch and Dittmar, 2006).

Considering the difference in the relative abundance, which are indicated by the difference in signal intensity in the mass spectrum of each formula in the sample, the average elemental ratios of oxygen, carbon, and hydrogen (i.e., O/C, H/C, etc.) and other characteristic parameters were calculated using the relative abundance weight following Song et al. (2018):

$$O/C_w = \Sigma(O/C_i \times Int_i)/\Sigma Int_i$$

$$H/C_w = \Sigma(H/C_i \times Int_i)/\Sigma Int_i$$

$$DBE_w = \Sigma(DBE_i \times Int_i)/\Sigma Int_i$$

$$OS_{Cw} = \Sigma(OS_{Ci} \times Int_i)/\Sigma Int_i$$

where Int_i represents the intensity of the mass spectrum for each individual molecular formula, *i*.

Cloud water samples were also analyzed for ionic species. Descriptions of these analyses are available elsewhere (Guo et al., 2012; Bianco et al., 2018). Briefly, water-soluble inorganic ions and oxalate ($C_2O_4^{2-}$) were detected using an ion chromatograph (883 Basic IC plus, Metrohm, Switzerland) with suppressed conductivity detection and a Metrosep C4-150/4.0 column (Metrohm) for cations and a Metrosep A Supp 5-150/4.0 column (Metrohm) for anions.

To obtained the concentration of water-soluble organic nitrogen (WSON) in cloud water, water soluble total nitrogen (WSTN) was analyzed using a TOC/TN analyzer (Vario, Elementar, Gemany). Water soluble inorganic nitrogen was calculated by summing mass of N in NH_4^+, NO_3^- and NO_2^-. Thus the concentration of WSON could be calculated as follow:

$$[WSON] = [WSTN] – ([NH_4^+\text{-}N] + [NO_3^-\text{-}N] + [NO_2^-\text{-}N])$$

where square brackets represent the concentration, NH_4^+-N represents nitrogen in NH_4^+ ion. The same is true for NO_3^--N and NO_2^--N.

Text S4. Meteorological conditions and water-soluble ions in cloud water

During the investigated period (May 11-12), air masses from the South China Sea and Southeast Asia and across Hainan Island and the boundary between Guangdong and Guangxi Provinces were dominant, according to the back-trajectory analysis (Fig. S1). As presented in Fig. S2, there is no obvious diurnal variation of temperature (15.2 -15.9 °C). As expected, the relative humidity was stable, with a constant value of 100%. The wind with speeds ranged from 3.3 to 7.5 m s^{-1}, primarily from the southwest. The $PM_{2.5}$ concentration varied from 2.0 to 4.3 μg m^{-3}, much lower than that in most urban areas in southern China. The NO_x, O_3, and SO_2 concentrations ranged from 2.2 to 7.7 μg m^{-3}, 60.6 to 101.0 μg m^{-3}, and 0.2 to 0.8 μg m^{-3}, respectively. The NO_x and O_3 concentrations showed a clear diurnal variation. Both of them were relatively stable in the daytime (approximately 2-4 μg m^{-3} and 85-100 μg m^{-3} for NO_x and O_3, respectively). However, NO_x reached a peak of 8 μg m^{-3} at approximately 01:00 LT, May 12, and then decreased, whereas O_3 dropped from approximately 100 μg m^{-3} at about 21:00, May 11 to 60 μg m^{-3} in the next morning (Fig. S2).

The concentrations of inorganic ions in the cloud water are listed in Table S1. Na^+, NH_4^+, K^+, Ca^{2+}, Mg^{2+}, Cl^-, NO_3^-, and SO_4^{2-} were detected. SO_4^{2-}, NO_3^-, and NH_4^+ were dominant, with average concentrations of 3.53, 2.88, and 1.11 mg L^{-1}, respectively; together they contributed approximately 90% of the total water-soluble inorganic ions. These concentrations are comparable to those observed in cloud water collected at Mt. Heng (Sun et al., 2010) and Mt. Lu (Sun et al., 2016) in southern China, but much lower than those observed at Mt. Tai in northern China (Guo et al., 2012). The average concentrations of SO_4^{2-}, NO_3^-, and NH_4^+ in the nighttime samples (4.34, 3.49, and 1.46 mg L^{-1}, respectively) were much higher than those in the daytime samples (2.71, 2.27, and 0.77 mg L^{-1}, respectively) (Table S1).

Text S5. Diurnal variation of WSON in cloud water

The long-duration cloud event lasted from May 8 to May 13, 2018. A total of 24 samples were collected. No sample was collected during the night between May 9 and 10. Note that the first sample CL1 and the last sample CL24 were not considered for the chemical analysis since these two samples were collected during the formation and dissipation stage of the long-duration cloud event, when the liquid water content is quite low and unstable compared with the normal cloud water. For the remaining samples CL2 to CL23, we divided them into five diurnal cycles based on the sampling duration, each day or night contained one to three sample(s) (Table S2). the concentration of WSON is generally low, with an average value of 0.55 mgN L^{-1}. Samples collected during the nighttime show a generally higher concentration of WSON compared with that during the daytime (Fig. S3). This phenomenon clearly shows that nocturnal cloud droplets contain more N-containing organic compounds, indicating the dark reactions may favor the formation of N-containing organics.

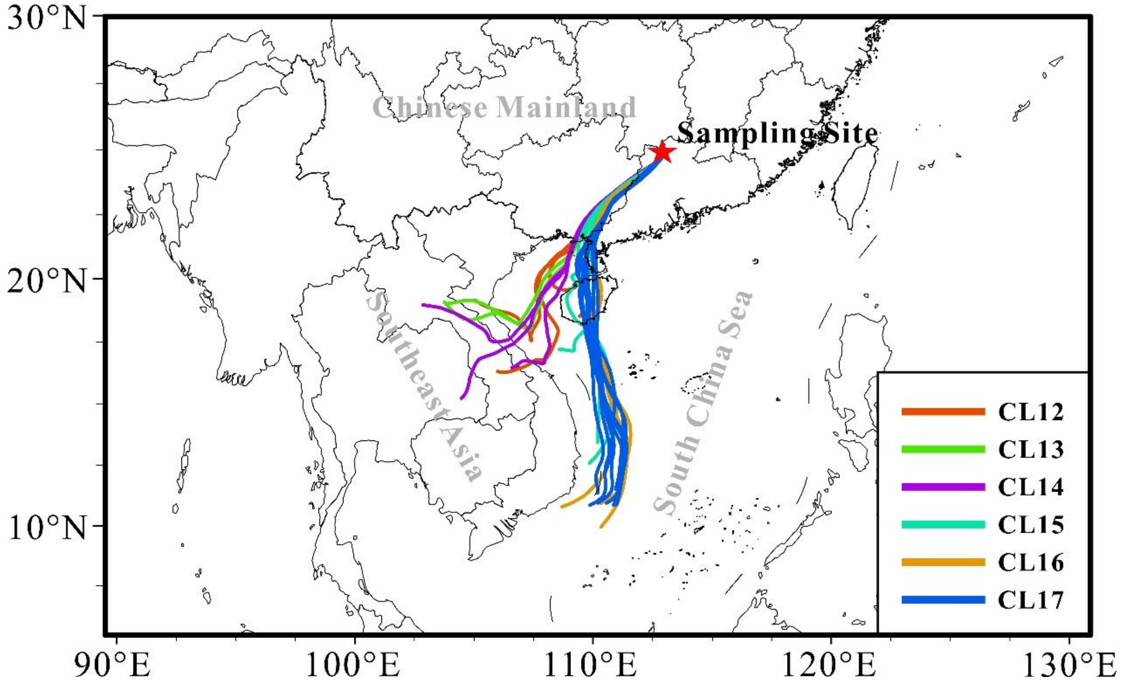

Figure S1. The location of the sampling site and 72 h back trajectories displayed by the Hybrid Single-Particle Lagrangian Integrated Trajectory model for every hours during sampling time (May 11 10:00 – May 12 08:00 LT).

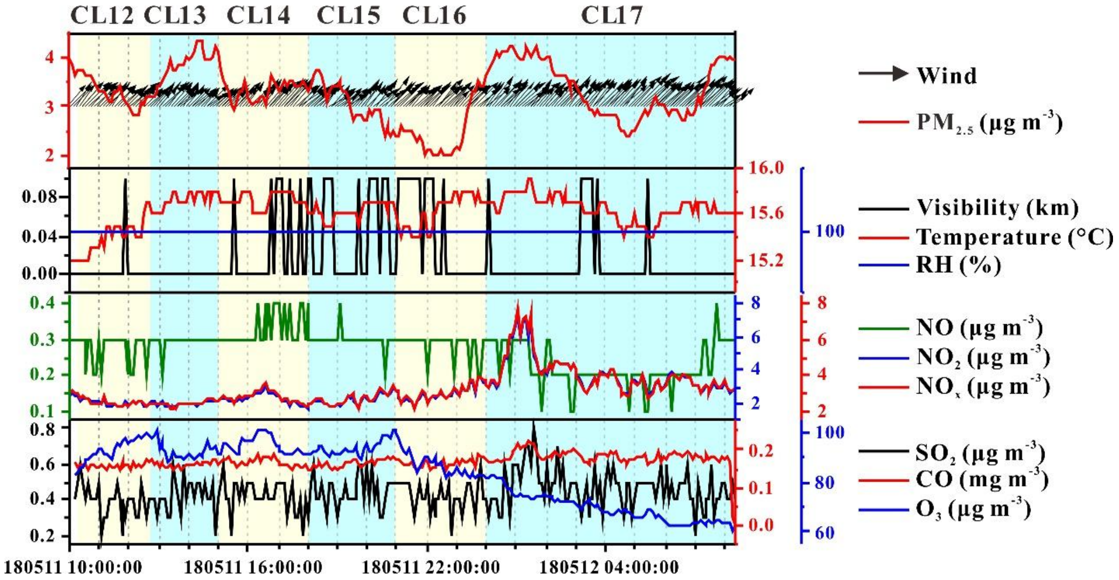

Figure S2. The time series of the meteorological data including visibility, temperature, relative humidity, concentration of some contaminant in the atmosphere (NO, NO$_2$, NO$_x$, SO$_2$, CO, and O$_3$). The data was obtained from Guangdong Environmental Monitoring Center. The alternating color lumps in the figure represent the duration of sampling.

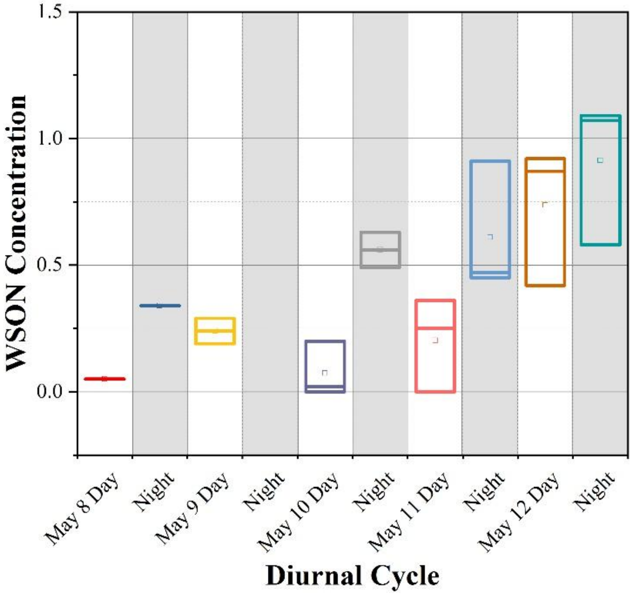

Figure S3. The diurnal variation of WSON concentrations in cloud water collected during the long-duration cloud event (from May 8 day to May 12 night).

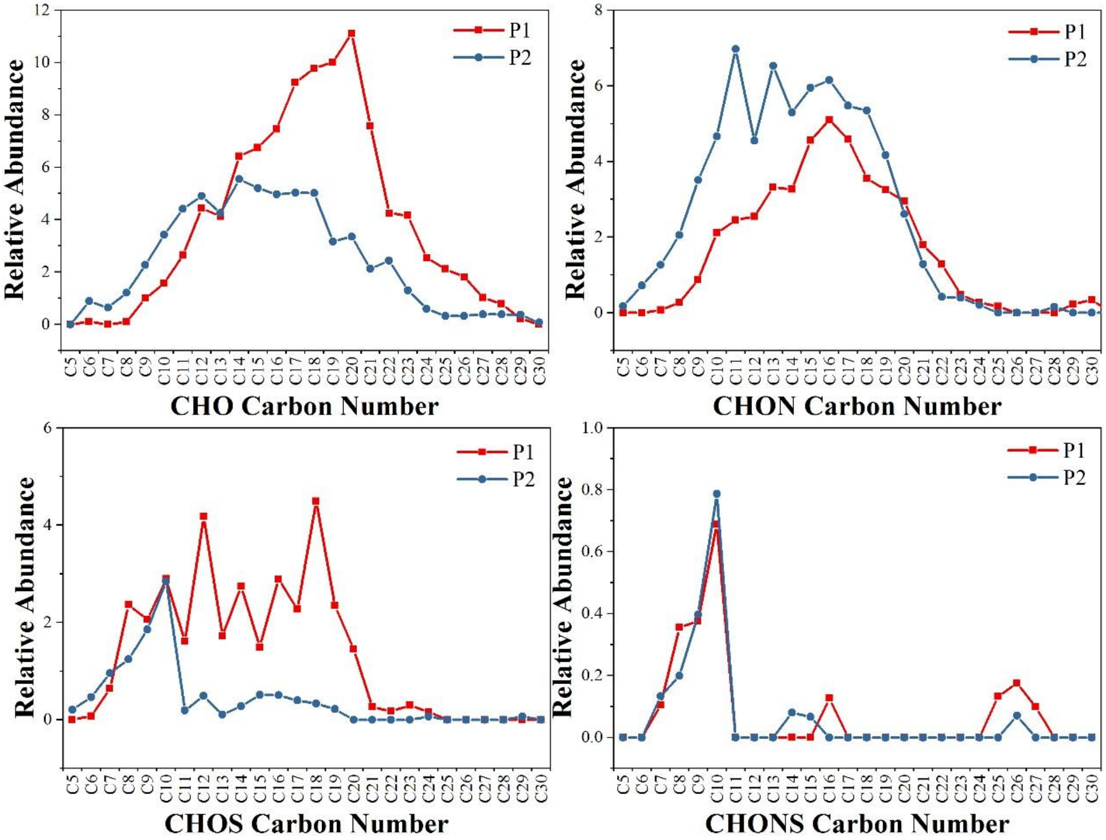

Figure S4. **The relative abundances with respect to the carbon atom number within four groups (CHO, CHON, CHOS and CHONS) of the molecular formulas in two PM$_{2.5}$ samples (P1 and P2).**

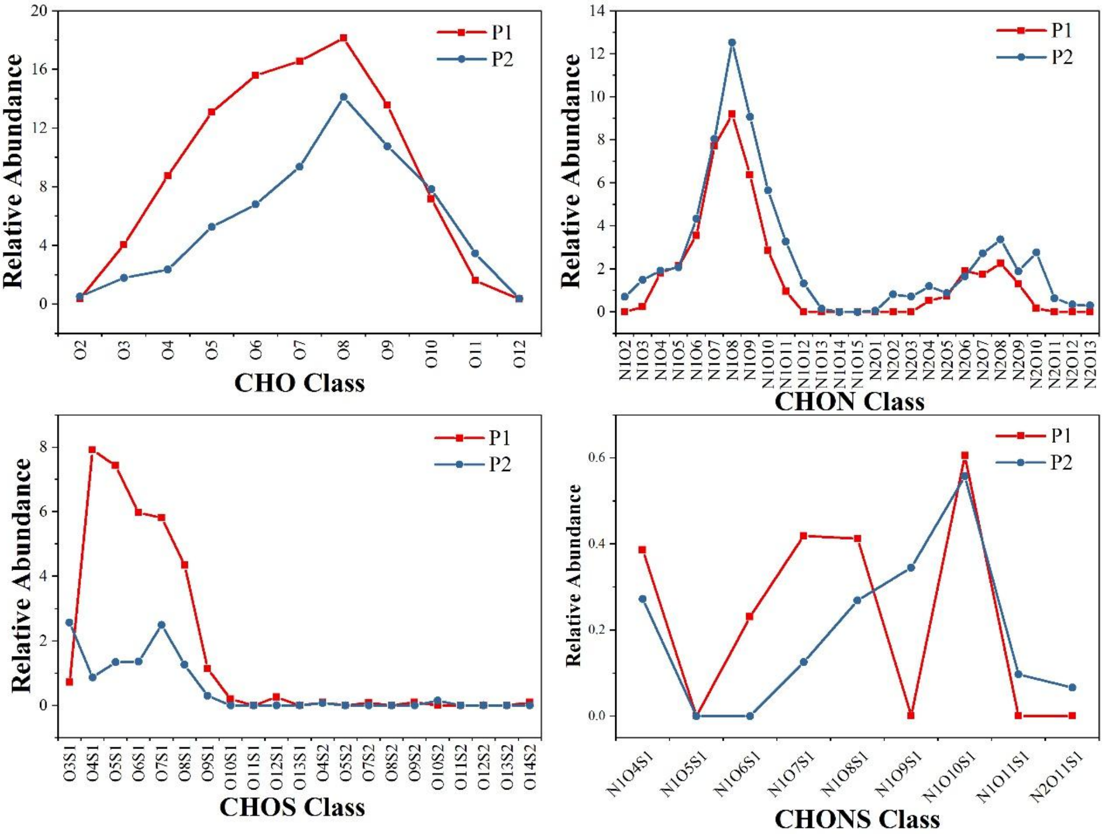

Figure S5. Relative abundance of the categories of CHO, CHON, CHOS and CHONS compounds according to the characteristic atom groups in the molecular formulas in two $PM_{2.5}$ samples (P1 and P2).

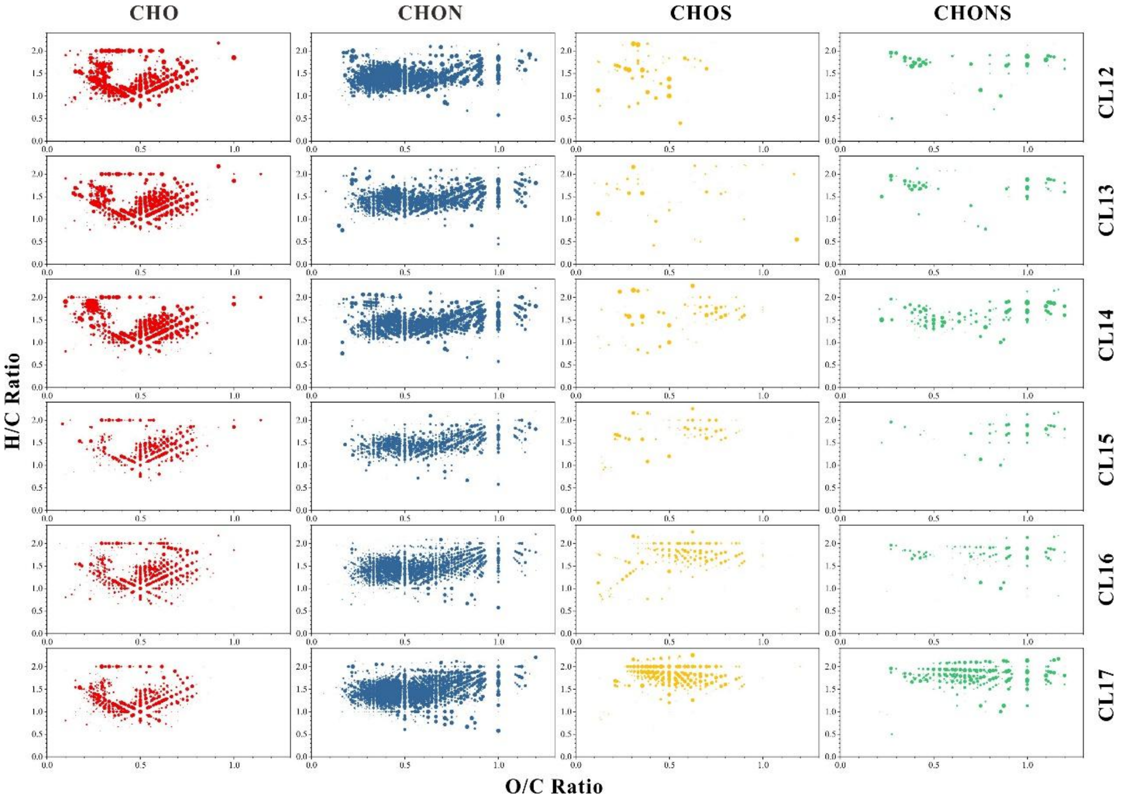

Figure S6. Van Krevelen diagrams as a function of four groups (CHO, CHNO, CHOS, and CHNOS) for the cloud water samples. The larger point in the diagram represents the higher relative abundance of the formula.

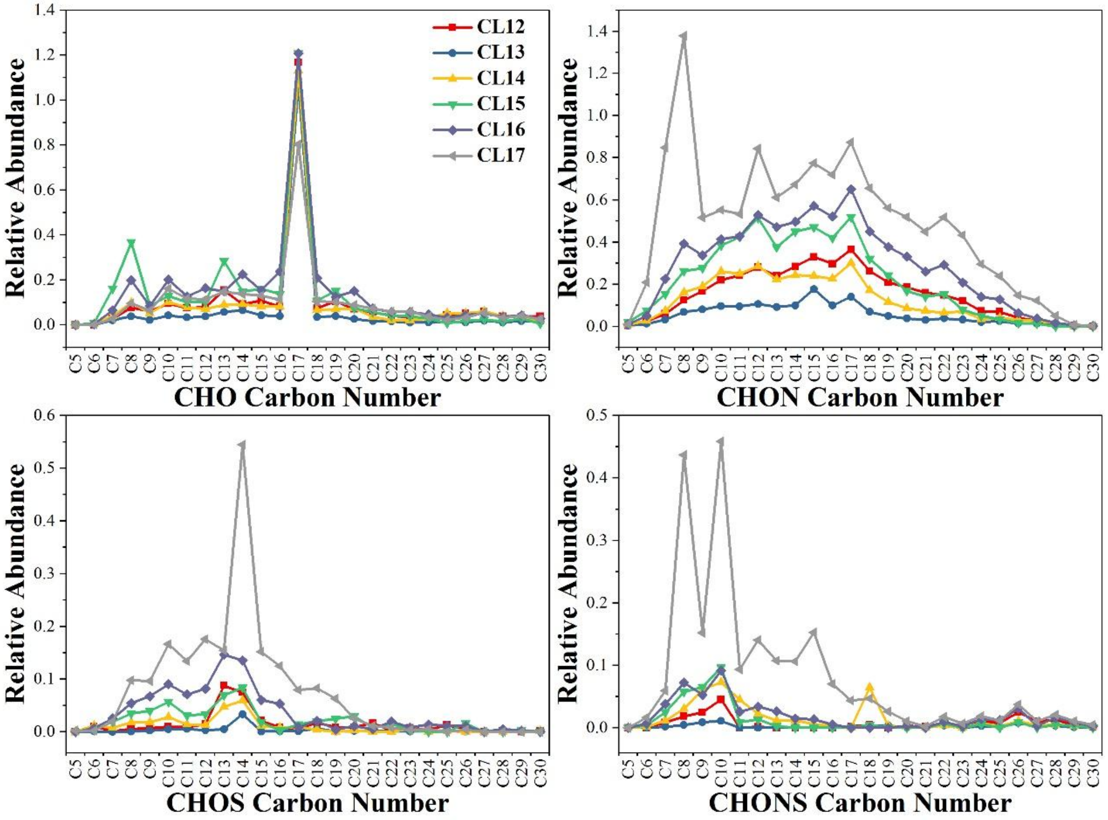

Figure S7. The relative abundances with respect to the carbon atom number within four groups (CHO, CHON, CHOS and CHONS) of the molecular formulas in the cloud water samples.

Table S1. The concentration of water-soluble inorganic ions in cloud water. The unit of the data is mg L^{-1}.

Sample ID	Na^+	NH_4^+	K^+	Mg^{2+}	Ca^{2+}	Cl^-	NO_3^-	SO_4^{2-}	$C_2O_4^{2-}$
CL12	0.17	0.61	0.04	0.04	0.01	0.34	2.21	2.66	0.19
CL13	0.27	0.80	0.09	0.03	0.02	0.27	2.30	2.74	0.30
CL14	0.23	0.91	0.05	0.03	0.00	0.27	2.30	2.74	0.47
CL15	0.29	1.23	0.08	0.05	0.04	0.37	3.11	4.05	0.39
CL16	0.25	1.46	0.09	0.05	0.03	0.46	3.44	4.23	0.06
CL17	0.37	1.69	0.10	0.06	0.03	0.67	3.93	4.74	N.D.

N.D.: Not detected.

Table S2. The sampling duration, liquid water content (LWC, g m^{-3}), and concentration of WSON (mgN L^{-1}) of the 24 samples during the cloud event from May 8 to May 13. The light blue and light grey tables represent the samples were collected during the day and night, respectively.

Sample ID	Start Time	End Time	LWC	WSON
CL1	2018/5/8 11:08	2018/5/8 18:13	0.10	--
CL2	2018/5/8 18:42	2018/5/8 21:01	0.15	0.05
CL3	2018/5/8 21:01	2018/5/9 9:46	0.05	0.34
CL4	2018/5/9 10:28	2018/5/9 13:20	0.11	N.D.
CL5	2018/5/9 14:00	2018/5/9 17:38	0.14	0.29
CL6	2018/5/9 17:40	2018/5/9 19:47	0.17	0.19
CL7	2018/5/10 8:15	2018/5/10 11:05	0.14	0.20
CL8	2018/5/10 11:05	2018/5/10 14:21	0.18	0.00
CL9	2018/5/10 16:07	2018/5/10 20:57	0.08	0.02
CL10	2018/5/10 21:00	2018/5/11 0:40	0.14	0.63
CL11	2018/5/11 0:40	2018/5/11 8:40	0.10	0.49
CL12	2018/5/11 10:15	2018/5/11 12:40	0.17	0.00
CL13	2018/5/11 12:40	2018/5/11 15:00	0.17	0.25
CL14	2018/5/11 15:00	2018/5/11 18:00	0.19	0.36
CL15	2018/5/11 18:00	2018/5/11 21:00	0.17	0.45
CL16	2018/5/11 21:00	2018/5/12 0:00	0.16	0.47
CL17	2018/5/12 0:00	2018/5/12 8:15	0.12	0.91
CL18	2018/5/12 8:15	2018/5/12 10:03	0.23	0.42
CL19	2018/5/12 10:28	2018/5/12 13:30	0.16	0.87
CL20	2018/5/12 13:30	2018/5/12 18:00	0.08	0.92
CL21	2018/5/12 18:00	2018/5/12 21:00	0.13	1.09
CL22	2018/5/12 21:00	2018/5/13 4:30	0.13	1.07
CL23	2018/5/13 4:30	2018/5/13 8:50	0.24	0.58
CL24	2018/5/13 8:53	2018/5/13 11:15	0.10	--

N.D.: Not detected.

Table S3. The number fraction and relative abundance fraction of four groups (CHO, CHON, CHOS, and CHONS) in two $PM_{2.5}$ samples.

Sample ID	Number Fraction				Relative Abundance Fraction			
	CHO	CHON	CHOS	CHONS	CHO	CHON	CHOS	CHONS
P1	49.8%	31.8%	17.2%	1.2%	55.5%	24.3%	19.1%	1.2%
P2	39.9%	51.0%	7.5%	1.6%	44.0%	47.3%	7.5%	1.2%

Table S4. The relative-abundance-weighted average values of O/C, H/C, DBE, OS_C and for all formulas, CHO, CHON, CHOS and CHONS formulas in two $PM_{2.5}$ samples (P1 and P2).

Group	Sample ID	O/C_w	H/C_w	DBE_w	OS_{Cw}
All	P1	0.45	1.53	5.04	-0.84
	P2	0.56	1.40	4.74	-0.61
CHO	P1	0.40	1.49	5.48	-0.69
	P2	0.53	1.45	5.03	-0.40
CHON	P1	0.53	1.51	5.32	-0.89
	P2	0.63	1.49	5.04	-0.75
CHOS	P1	0.46	1.65	3.49	-1.19
	P2	0.61	1.39	4.73	-0.83
CHONS	P1	0.66	1.69	3.22	-1.40
	P2	0.86	1.74	2.98	-1.17

Table S5. The number fraction and relative abundance fraction of four groups (CHO, CHON, CHOS, and CHONS) in each cloud water sample.

Sample ID	Number Fraction				Relative Abundance Fraction			
	CHO	CHON	CHOS	CHONS	CHO	CHON	CHOS	CHONS
CL12	26.6%	65.2%	4.5%	3.7%	37.6%	54.9%	4.7%	2.7%
CL13	28.3%	64.4%	3.6%	3.7%	52.1%	43.6%	2.3%	2.0%
CL14	27.1%	60.2%	4.9%	7.8%	39.3%	50.5%	4.1%	6.1%
CL15	23.5%	66.2%	6.4%	3.9%	35.3%	56.2%	5.3%	3.1%
CL16	21.7%	65.4%	8.1%	4.8%	30.0%	58.9%	7.3%	3.9%
CL17	16.3%	65.1%	9.4%	9.3%	13.8%	65.3%	10.2%	10.8%

Table S6. The values of average O/C, H/C, DBE, number of carbon (#C) and OS_C and relative-abundance-weighted values of that for all formulas, CHO, CHON, CHOS and CHONS compounds in cloud water.

All

Sample ID	O/C	H/C	DBE	#C	OS_C	O/Cw	H/Cw	DBEw	#Cw	OS_{Cw}
CL12	0.46	1.44	6.16	16.92	-0.88	0.45	1.47	5.70	16.16	-0.87
CL13	0.52	1.45	5.96	16.31	-0.76	0.45	1.48	5.37	15.82	-0.81
CL14	0.53	1.46	5.61	15.91	-0.82	0.51	1.48	5.25	15.22	-0.79
CL15	0.56	1.47	5.61	15.20	-0.76	0.56	1.49	5.10	14.38	-0.72
CL16	0.52	1.46	5.92	16.47	-0.83	0.54	1.48	5.41	15.28	-0.79
CL17	0.51	1.49	5.86	16.80	-0.92	0.55	1.44	5.44	14.58	-0.91

CHO

Sample ID	O/C	H/C	DBE	#C	OS_C	O/Cw	H/Cw	DBEw	#Cw	OS_{Cw}
CL12	0.41	1.38	6.37	18.18	-0.57	0.36	1.45	5.59	16.98	-0.72
CL13	0.46	1.38	6.30	17.67	-0.46	0.34	1.47	5.33	16.69	-0.80
CL14	0.44	1.41	5.82	17.98	-0.53	0.38	1.46	5.29	16.78	-0.71
CL15	0.50	1.39	5.79	15.93	-0.39	0.46	1.47	4.96	14.94	-0.54
CL16	0.47	1.36	6.35	17.53	-0.41	0.45	1.46	5.27	16.11	-0.56
CL17	0.43	1.31	6.85	17.50	-0.46	0.39	1.36	6.12	16.44	-0.58

CHON

Sample ID	O/C	H/C	DBE	#C	OS_C	O/Cw	H/Cw	DBEw	#Cw	OS_{Cw}
CL12	0.48	1.45	6.24	16.46	-0.98	0.51	1.45	6.00	15.65	-0.92
CL13	0.54	1.45	5.99	15.66	-0.86	0.59	1.48	5.50	14.75	-0.78
CL14	0.55	1.46	5.84	15.64	-0.87	0.60	1.46	5.50	14.46	-0.76
CL15	0.57	1.47	5.81	15.25	-0.84	0.62	1.48	5.44	14.27	-0.76
CL16	0.53	1.46	6.24	16.60	-0.90	0.57	1.44	5.88	15.23	-0.83
CL17	0.50	1.46	6.41	17.31	-0.94	0.56	1.37	6.09	14.77	-0.87

CHOS

Sample ID	O/C	H/C	DBE	#C	OS_C	O/Cw	H/Cw	DBEw	#Cw	OS_{Cw}
CL12	0.39	1.56	4.92	16.20	-1.22	0.36	1.66	3.87	15.11	-1.39

CL13	0.50	1.58	4.75	16.16	-1.03	0.45	1.56	4.58	15.15	-1.11
CL14	0.59	1.58	3.81	12.35	-0.99	0.50	1.66	3.19	12.60	-1.21
CL15	0.50	1.61	4.35	13.93	-1.11	0.47	1.68	3.72	13.77	-1.23
CL16	0.52	1.65	3.64	13.74	-1.09	0.51	1.71	3.21	13.27	-1.18
CL17	0.50	1.74	2.89	14.10	-1.21	0.48	1.75	2.72	13.43	-1.27
CHONS										
Sample ID	O/C	H/C	DBE	#C	OS_C	O/Cw	H/Cw	DBEw	#Cw	OS_{Cw}
CL12	0.68	1.63	4.63	17.03	-1.14	0.69	1.67	4.29	16.96	-1.19
CL13	0.67	1.71	4.12	17.42	-1.21	0.67	1.71	4.13	17.28	-1.21
CL14	0.67	1.58	4.22	13.10	-1.31	0.65	1.60	4.25	13.22	-1.33
CL15	0.84	1.72	3.18	11.98	-1.15	0.88	1.72	3.01	10.92	-1.14
CL16	0.74	1.71	3.48	14.47	-1.17	0.78	1.68	3.42	13.33	-1.16
CL17	0.70	1.77	3.29	14.75	-1.27	0.78	1.70	3.19	12.09	-1.21

Table S7. The fraction in relative abundance of aliphatic/olefinic and (condensed) aromatic structures in cloud water.

CHO

Sample ID	CL12	CL13	CL14	CL15	CL16	CL17
Aliphatic/Olefinic	95.8%	98.3%	97.1%	97.2%	94.9%	98.2%
(Condensed) Aromatic	4.2%	1.7%	2.9%	2.8%	5.1%	1.8%

CHON

Sample ID	CL12	CL13	CL14	CL15	CL16	CL17
Aliphatic/Olefinic	96.1%	97.5%	97.2%	97.1%	92.5%	79.2%
(Condensed) Aromatic	3.9%	2.5%	2.8%	2.9%	7.5%	20.8%

CHOS

Sample ID	CL12	CL13	CL14	CL15	CL16	CL17
Aliphatic/Olefinic	93.9%	95.3%	96.3%	93.5%	95.7%	98.8%
(Condensed) Aromatic	6.1%	4.7%	3.7%	6.5%	4.3%	1.2%

CHONS

Sample ID	CL12	CL13	CL14	CL15	CL16	CL17
Aliphatic/Olefinic	95.7%	98.2%	100.0%	100.0%	98.6%	99.6%
(Condensed) Aromatic	4.3%	1.8%	0.0%	0.0%	1.4%	0.4%